

# Design and Simulation of a Doherty-mode OLMBA for Enhanced Back-Off Efficiency Over an Octave Bandwidth

Jean-Baptiste Urvoy, Roberto Quaglia, Steve C. Cripps

Cardiff University, Cardiff, UK. E-mail: UrvoyJ@cardiff.ac.uk

**Abstract**—This paper presents a new design for the OLMBA focused on exploiting a Doherty-like mode with one device in class AB and the other in class C to enhance 6 dB output back-off efficiency across an octave bandwidth of 0.8 to 1.6 GHz. The simulation results show that the device can achieve 48 to 53 % back-off PAE while delivering an output power of 46 to 48 dBm at 3 dB compression and 12.6 to 16.1 dB gain. Furthermore, the operation of this device seems to conform with the operation of Doherty power amplifiers in terms of how the intrinsic impedance changes between back-off and saturation. Whilst this is only based on simulated results, it does show that it is a promising design for a high-efficiency, wide-bandwidth OLMBA for linear applications.

**Index Terms**—Power Amplifiers, Tunable Load Modulation, Load Modulated Balanced Amplifier, Doherty Power Amplifier, Back Off Efficiency

## I. INTRODUCTION

Due to the ever-increasing complexities of modern communication standards, new power amplifier (PA) architectures must be able to handle greater bandwidths and peak-to-average power ratios (PAPR) while still exhibiting good linearity and efficiencies. The Doherty power amplifier (DPA) remains the most popular PA architecture for base station applications because of its high output back-off (OBO) efficiency, making it suitable for high PAPR signals [1]. This device achieves this performance by using an auxiliary device in class C to “linearise” the main device in class AB when it goes into compression. The power from these two devices is combined through an inverting transformer. As communication standards become more sophisticated as we move past 5G and into 6G and beyond, there is an increasing demand for highly reconfigurable power amplifiers to surpass existing ‘fixed state’ amplifiers. However, the inverting transformer poses an inherent physical limitation to the bandwidth and reconfigurability of the DPA.

The load modulated balanced amplifier (LMBA) [2] has been shown to have a very good performance as a highly wideband device. By changing the control signal (CSP) to the device the load presented to the amplifier can be controlled – unlike in the DPA – satisfying the desire for reconfigurable PAs. However, the LMBA is limited in OBO extension making it unsuitable for telecoms applications. Furthermore, the LMBA has some issues with the generation of the CSP. Many

new architectures have been developed to improve upon the original LMBA to enhance the OBO range and improve the linearity.

One such architecture is the orthogonal LMBA (OLMBA) [3]. This device was initially developed to address the issues brought about by the generation of the CSP. By injecting the CSP on the input side of the device, the CSP can be amplified by the balanced amplifier itself and then reflected off a reactive  $jX$  termination on the isolated output port to provide the load modulation. Not only does this method enhance the bandwidth compared to the LMBA, but also mitigates load mismatch effects [4]. Previous work showed the possibility of enhancing the OLMBA’s OBO efficiency by operating it in a Doherty-like mode – with one device in class AB and the other in class C [5]. This work was done on an existing OLMBA device that was not originally designed for this mode of operation, but it showed an OBO efficiency of 35 to 50 % across an 85.7 % bandwidth. The paper presents a brand new device designed specifically for Doherty-like operation with the primary goal of improving 6 dB OBO performance.

Currently in the literature, novel devices operating around L and S bands typically show OBO efficiencies of around 35 to 60 % for output powers ranging from around 42 to 48 dBm and bandwidths around 20 to 50 % [6] [7] [8]. Naturally, there are outliers, however this provides a benchmark for comparison for this paper and the Doherty-mode OLMBA.

## II. DESCRIPTION OF THE DEVICE

A block diagram of the device is shown in Fig. 1.

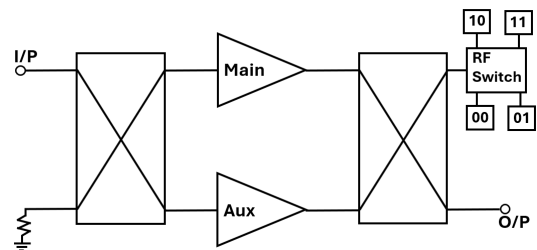


Fig. 1. Block diagram of Doherty-mode OLMBA.

Traditionally, LMBA and their derivative devices are balanced amplifiers at their core. In the OLMBA, the load modulation is achieved by unbalancing the signals at the output of the two devices by injecting a relatively small CSP signal on the input isolated port which is orthogonal to the main signal. In the Doherty-mode OLMBA, the unbalancing is achieved by biasing the auxiliary device in class C, eliminating the need for the CSP signal.

Both the main and auxiliary devices are CG2H40025 25 W GaN amplifiers. The output coupling is achieved by an IPP-7048 800 to 1600 MHz coupler, while the input coupling is achieved by an IPP-7036 1700 to 2200 MHz coupler. This out-of-band coupler provides an uneven input power splitting that ensures that more power goes to the auxiliary device, a common practice in DPA design to ensure optimum load modulation [9] [10]. The amplitude balance of the IPP-7036 at the selected frequencies is displayed in Fig. 2.

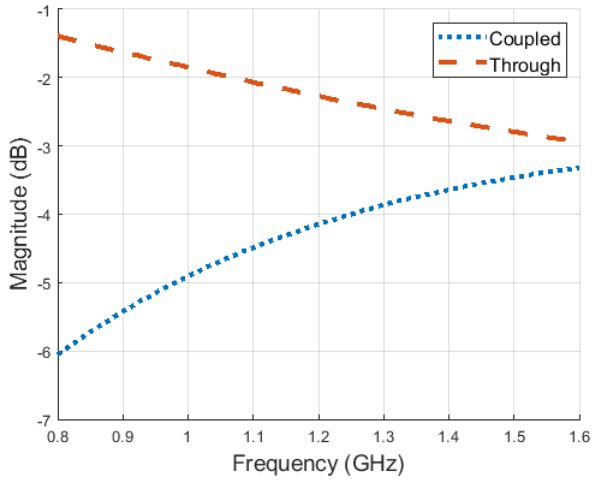


Fig. 2. Amplitude of the through and coupled outputs of the IPP-7036 hybrid coupler at the design frequency.

The reflective  $jX$  port is controlled by the measured S-parameters of an ADRF5347 4 port CMOS RF switch with the four ports connected to different reactive terminations. The values of the reactive loads are chosen to be approximately equidistant to each other around the edge of the Smith chart.

### III. SIMULATION RESULTS

#### A. Simulation of Doherty-like Intrinsic Impedance

Typically in DPAs, the intrinsic impedance of the main device is twice the optimum at OBO and moves to the optimum at saturation with the impedance of the auxiliary going from an infinite impedance to the optimum [11]. For the Doherty-mode OLMBA to exhibit Doherty behaviour its impedance should follow a similar trajectory. The impedance at OBO is dependent on  $jX$  because at OBO the unbalancing of the two devices is strongest. Therefore,  $jX$  can be used to adjust the OBO impedance over frequency. Frequency by frequency, the optimum  $jX$  can be identified by sweeping the value of the phase of its reflection coefficient. This can be done

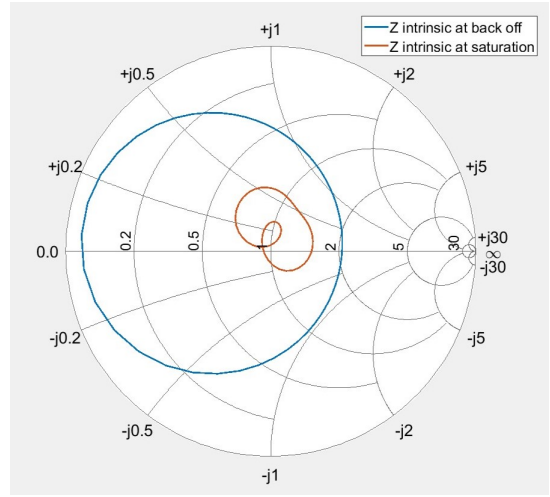


Fig. 3. Impedance presented to main device at Back of and at saturation as the phase of the reflection coefficient of  $jX$  is swept from 0 to 355 degrees at 1.2 GHz. Smith chart normalised to  $12\Omega$

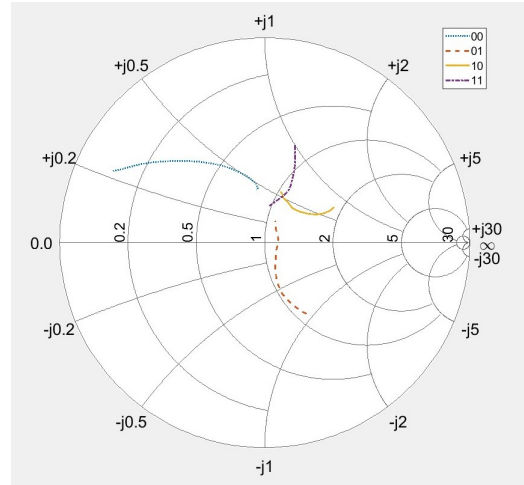


Fig. 4. Intrinsic impedance of main device as power is swept from back off to saturation for four  $jX$  switch conditions at 1.2 GHz. Smith chart normalised to  $12\Omega$

by replacing the RF switch with a one port S parameter block and sweeping the phase of the  $jX$ . As an example, Fig 3 shows the results of this sweep at 1.2 GHz in terms of the intrinsic device impedance at OBO and saturation. The optimum phase for Doherty behaviour is at the point where the OBO phase sweep crosses the origin at twice the optimum impedance.

The RF switch can be reintroduced and the input power swept under each switch condition at 1.2 GHz. The intrinsic impedances are shown in Fig. 4. As shown, as the four switch states are swept four different traces of impedance are shown at approximately 90 degrees from each other. The one closest to the Doherty behaviour – state 10 – can be assumed to be the best state for OBO performance, and this will be further illustrated in the following section.

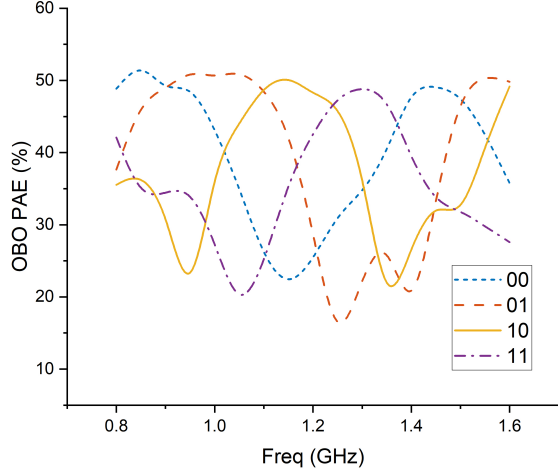


Fig. 5. OBO PAE across frequency under each switch condition

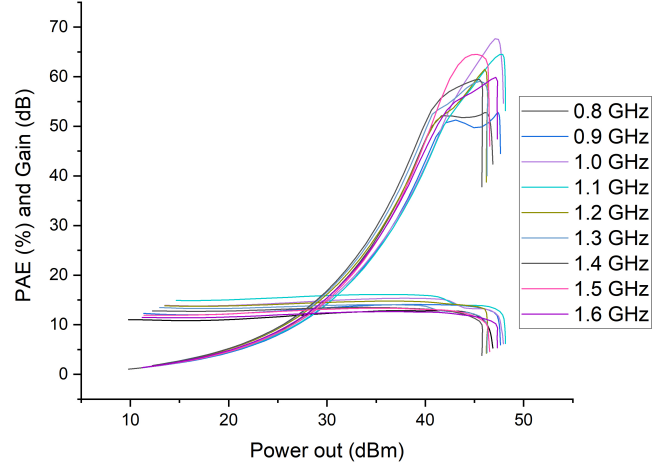


Fig. 7. Gain and PAE at all frequencies as power is swept

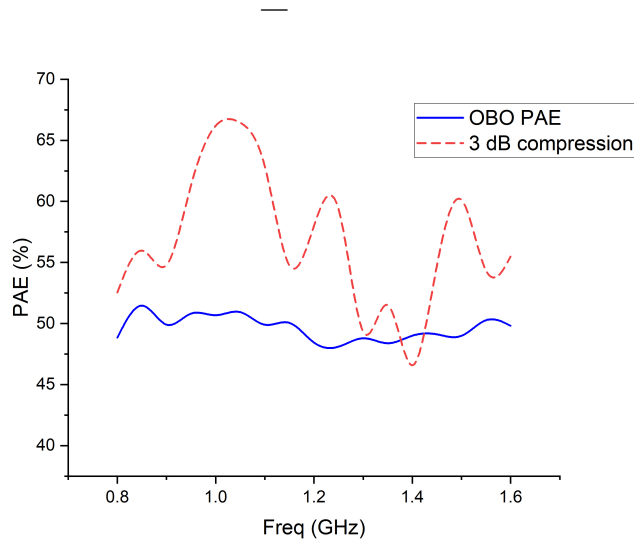


Fig. 6. Output back off and saturation PAE with optimum parameters

### B. CW Simulation Results

The CW input power to the OLMBA was swept under each switch condition and the OBO PAE at each state is shown in Fig. 5. The values of OBO PAE are evaluated at an output power 6 dB less than the output power at 3 dB gain compression. As shown, the switch state - and, therefore, the load modulation - strongly affects the performance. Notably, at 1.2 GHz, it can be observed that the switch state that provides the best performance is the 10 state and the worst is state 00, which conforms to the findings in Fig. 4 where the 10 state most closely follows the Doherty load trajectory whereas the 00 state is on the opposite side of the smith chart.

The OBO and saturation efficiency at each frequency and under the optimum switch state are shown in Fig. 6 and the

PAE and gain for each power sweep with the optimum switch state are shown in Fig. 7. As shown, the PAE for the Doherty-mode OLMBA closely resembles the Doherty efficiency curve with a peak at saturation and a peak at 6 dB of OBO. Those figures show that the OBO efficiency is around 48 to 53%, the gain is 12.6 to 16.1 dB and the output power at 3 dB compression is between 46 and 48 dBm across the full octave bandwidth. As a point of comparison with other work in the literature, the OBO PAE is on par with other devices; however, these results also suggest the ability of the presented device to achieve this with better bandwidth at a relatively high output power.

## IV. CONCLUSIONS

TABLE I  
COMPARISON TO STATE OF THE ART

Ref.	Freq.(GHz)	Pout(dBm)	DE(OBO%)
[6]	1.65-1.9/2.65-2.75	45.5-46.8	42.3-62 <sup>§</sup>
[7]	2	46.4-46.7	62.8-60.7 <sup>#</sup>
[8]	1.5-2.3	44.8-45.6	40-60*
[12]	2.4	45.6	54*
[13]	1.7-2.2	42-43.5	49.8-60.2*
[14]	1.5-2.7	43	47-61*
This	0.8-1.6	46-48	48-53 (PAE)*

<sup>§</sup>9.5dB; <sup>#</sup>9dB; \*6dB

The design and simulated results for a Doherty-mode OLMBA for improved OBO efficiency have been demonstrated. By combining design concepts from both LMBA and DPA, a wideband reconfigurable device with high OBO efficiency is achievable. Further work is required to fully implement this device, including manufacturing and characterising it experimentally. Furthermore, experimental characterisation should include modulated measurements to demonstrate further this device's capabilities as a possible alternative for telecom applications.

## REFERENCES

- [1] X. Y. Zhou, W. S. Chan, S. Chen, and W. J. Feng, "Broadband highly efficient Doherty power amplifiers," *IEEE Circuits and Systems Magazine*, vol. 20, no. 4, pp. 47–64, 2020.
- [2] D. J. Sheppard, J. Powell, and S. C. Cripps, "An efficient broadband reconfigurable power amplifier using active load modulation," *IEEE Microw. Wireless Compon. Lett.*, vol. 26, no. 6, pp. 443–445, Jun. 2016.
- [3] D. J. Collins, R. Quaglia, J. R. Powell, and S. C. Cripps, "The orthogonal LMBA: A novel RFPA architecture with broadband reconfigurability," *IEEE Microw. Wireless Compon. Lett.*, vol. 30, no. 9, pp. 888–891, Sep. 2020.
- [4] R. Quaglia, J. R. Powell, K. A. Chaudhry, and S. C. Cripps, "Mitigation of load mismatch effects using an orthogonal load modulated balanced amplifier," *IEEE Trans. Microw. Theory Techn.*, vol. 70, no. 6, pp. 3329–3341, 2022.
- [5] J.-B. Urvoy, R. Quaglia, J. R. Powell, and S. C. Cripps, "Experimental characterization of a dual-input OLMBA for back-off efficiency improvement," in *2023 53rd European Microwave Conference (EuMC)*, 2023, pp. 267–270.
- [6] J. Wang, Z. Dai, K. Zhong, G. Bai, C. Bi, M. Li, W. Shi, and J. Pang, "Design of a dual-band Doherty power amplifier using single-loop network," *IEEE Transactions on Microwave Theory and Techniques*, vol. 72, no. 10, pp. 5818–5829, 2024.
- [7] J. Pang, Y. Han, J. Peng, M. Li, Z. Dai, W. Shi, X. Zhou, and A. Zhu, "Dual-mode three-way Doherty power amplifier with extended high-efficiency range against load mismatch," *IEEE Transactions on Microwave Theory and Techniques*, vol. 72, no. 7, pp. 4058–4067, 2024.
- [8] W. Shi, X. Li, C. Hu, P. Li, M. Sun, Z. Dai, J. Pang, and M. Li, "Design of broadband divisional load-modulated balanced amplifier with extended dynamic power range," *IEEE Transactions on Microwave Theory and Techniques*, vol. 72, no. 8, pp. 4638–4649, 2024.
- [9] J. Kim, J. Cha, I. Kim, and B. Kim, "Optimum operation of asymmetrical-cells-based linear Doherty power amplifiers-uneven power drive and power matching," *IEEE Transactions on Microwave Theory and Techniques*, vol. 53, no. 5, pp. 1802–1809, 2005.
- [10] P. Colantonio, F. Giannini, R. Giofrè, and L. Piazzon, "The AB-C Doherty power amplifier. Part I: Theory," *Int. J. RF Microw. Comput.-Aided Eng.*, vol. 19, no. 3, pp. 293–306, May 2009.
- [11] S. Cripps, *RF power amplifiers for wireless communications*, ser. Artech House Microwave Library. Artech House, 2006.
- [12] P. H. Pednekar, W. Hallberg, C. Fager, and T. W. Barton, "Analysis and design of a doherty-like rf-input load modulated balanced amplifier," *IEEE Transactions on Microwave Theory and Techniques*, vol. 66, no. 12, pp. 5322–5335, 2018.
- [13] Z. Fan, Z. Hao, J. Huang, and J. Cai, "Design of rf-input sequential lmbs using pso algorithm with improved linear self-adaptive hyperparameters," *IEEE Transactions on Microwave Theory and Techniques*, vol. 72, no. 11, pp. 6414–6425, 2024.
- [14] Y. Cao and K. Chen, "Pseudo-doherty load-modulated balanced amplifier with wide bandwidth and extended power back-off range," *IEEE Transactions on Microwave Theory and Techniques*, vol. 68, no. 7, pp. 3172–3183, 2020.